Internal strain and photoelastic effects in $Ga_{1-x}Al_xAs/GaAs$ and $In_{1-x}Ga_xAs_yP_{1-y}/InP$ crystals

Cite as: Journal of Applied Physics **54**, 6620 (1983); https://doi.org/10.1063/1.331898
Submitted: 27 April 1983 . Accepted: 06 July 1983 . Published Online: 04 June 1998

Sadao Adachi, and Kunishige Oe

Internal strain and photoelastic effects in $Ga_{1-x}Al_xAs/GaAs$ and $In_{1-x}Ga_xAs_yP_{1-y}/InP$ crystals

Sadao Adachi and Kunishige Oe
Musashino Electrical Communication Laboratory, Nippon Telegraph and Telephone Public Corporation, Musashino-shi, Tokyo 180, Japan

(Received 27 April 1983; accepted for publication 6 July 1983)

A method for calculation of photoelastic coefficients in III-V compounds at energies below the direct band edge is presented. Spectral dependence of the photoelastic-coefficient data is analyzed on the basis of simplified model of the interband transitions. The theoretical prediction shows a quite good agreement with the experimental data of III-V binaries. This model is applied to $Ga_{1-x}Al_xAs$ ternaries lattice-matched to GaAs and to $In_{1-x}Ga_xAs_yP_{1-y}$ quaternaries lattice-matched to InP. A method for analysis of the internal-strain induced effects in elastically-deformed heterostructure crystals is also discussed in detail.

PACS numbers: 78.20.Hp, 78.20.Dj, 78.20.Fm, 62.20.Dc

I. INTRODUCTION

Investigation of the photoelastic (elasto-optic) behaviors in solids is an old topic which arises in strong connection with the fundamental optical properties of the solids.[1] Knowledge of the photoelastic behaviors of III-V compounds forms an important part not only in the analysis of heteroepitaxial wafers but also in the design of optoelectronic devices, such as light modulators, deflectors, and switches.

The distribution of stress in heteroepitaxial semiconductor structures is a subject of perennial, great interest since internal stresses arise normally in thin epitaxial films during preparation of the films by heteroepitaxial growth.[2] The stresses have an important influence on the physical properties of the films. Much attention has, therefore, been paid to calculate stress distributions in epitaxial structures[3,4] and, more recently, to heterojunction laser structures.[5,6] The subject of photoelasticity deals with the artificial birefringence developed in a solid under an application of the stress. This phenomenon has been applied by Reinhart and Logan[3] to analyze interface stress of GaAlAs–GaAs layer structures. They have demonstrated its elastic nature and its magnitude to be consistent with predictions from the different thermal expansion coefficients of the layers. It is noted that photoelasticity is a function of light wavelength (i.e., it has a wavelength dispersion).[1]

Kirkby *et al.*[7] have formed photoelastic waveguide in GaAlAs/GaAs by small variations of the refractive index of the active layer beneath the stripe contact of the laser. The refractive index variations are caused by the effect of a strain field in the semiconductor surrounding the stripe window. This strain field results from the highly compressed state of the deposited SiO_2/Si_3N_4 insulating films. Photoelastic coefficient is necessary in calculating the figure of merit for such optoelectronic devices.[8] The wavelength dispersion of the photoelastic coefficients in III-V compounds has been reported: GaAs,[9,10] GaP,[11,12] GaSb,[13] AlSb,[14] InAs,[13] InP,[12] and InSb.[13] However, there has been no detailed report on the subject for alloyed III-V compounds.

The purpose of this paper is twofold: (1) to present the wavelength dispersion of the photoelastic coefficients in $Ga_{1-x}Al_xAs$ ternaries and $In_{1-x}Ga_xAs_yP_{1-y}$ quaternaries, and (2) to demonstrate a method for analysis of the internal-strain-induced effects in heterostructure materials. The dielectric constant of a solid is, in general, dependent on the stress (strain) in the solid. This effect is called the photoelastic effect.[1] In Sec. II, we obtain theoretical expressions of both the dielectric constant and photoelastic coefficient. The approach is based on a simplified model of the interband transitions.[15] In order to confirm the validity of the present model, we compare our calculated results with the experimental photoelastic-coefficient data of some of the III-V binaries. The $Ga_{1-x}Al_xAs/GaAs$ and $In_{1-x}Ga_xAs_yP_{1-y}/InP$ systems are necessary for the efficient operation of a number of transport and optoelectronic devices, i.e., high-speed heterojunction transistors, lasers, photodetectors, etc. In Sec. III, our model will be successfully applied to $Ga_{1-x}Al_xAs$ ternaries lattice-matched to GaAs and to $In_{1-x}Ga_xAs_yP_{1-y}$ quaternaries lattice-matched to InP. Finally, in Sec. IV, the conclusions obtained in the present study are summarized.

II. THEORETICAL EXPRESSIONS

A. Dielectric constant

The fundamental optical excitation spectrum of a material can be described in terms of a frequency-dependent complex dielectric constant $\epsilon(\omega)$[16]:

$$\epsilon(\omega) = \epsilon_1(\omega) + i\epsilon_2(\omega), \tag{1}$$

where $\hbar\omega$ is the photon energy. The dielectric constant has well-known integral dispersion relations between the real and imaginary parts of the function $\epsilon(\omega)$ dependent on the frequency ω (Kramers–Kronig relations)[16]:

$$\epsilon_1(\omega) = 1 + \frac{2}{\pi}\int_0^\infty \frac{\omega'\epsilon_2(\omega')}{(\omega')^2 - \omega^2}\,d\omega', \tag{2a}$$

$$\epsilon_2(\omega) = -\frac{2}{\pi}\int_0^\infty \frac{\epsilon_1(\omega')}{(\omega')^2 - \omega^2}\,d\omega'. \tag{2b}$$

In the previous paper,[15] we presented a method for calculation of refractive indices in III-V compounds at energies below the direct band edge. Spectral dependence of the refrac-

 0021-8979/83/116620-08$02.40

tive index data was analyzed on the basis of simplified model of the interband transitions. The theoretical prediction showed a quite good agreement with the experimental data of III-V binaries and $In_{1-x}Ga_xAs_yP_{1-y}$ quaternaries. Since $\epsilon_2(\omega)$ may be taken as zero in the region near and below the lowest-direct gap, one can obtain the following relation:

$$\epsilon_1(\omega) \simeq n(\omega)^2, \tag{3}$$

where n is the frequency-dependent refractive index. The model dielectric constant can now be given by[15]

$$\epsilon_1(\omega) = \epsilon_1^{DG}(\omega) + \epsilon_{1\infty}, \tag{4}$$

where $\epsilon_1^{DG}(\omega)$ is a dispersive contribution arising from the M_0 critical point and $\epsilon_{1\infty}$ is a nondispersive contribution arising from other, far-off critical points in the band structure (such as E_1, $E_1 + \Delta_1$, and E_2 gaps). To obtain formulas of the dispersive contribution, we must consider two kinds of the interband transitions at the lowest-direct gap: one is the free electron-hole pair transition (band-to-band transition) and the other is the Wannier-exciton transition. If the exciton Rydberg energy is very small, one can rightly approximate that the contribution from the exciton transition becomes very small compared with that from the free electron-hole pair transition. This assumption is thought to be reasonable for the most III-V compounds, such as InP, InAs, and GaAs. Under this assumption, we obtain the expression of $\epsilon_1(\omega)$ in the photon energy below the lowest-direct gap E_0 as[15]

$$\epsilon_1(\omega) = A\{f(\chi) + 1/2[E_0/(E_0+\Delta_0)]^{3/2} f(\chi_{so})\} + B, \tag{5}$$

with

$$A = 4/3(3\mu/2)^{3/2}P^2, \tag{6}$$

$$f(\chi) = \chi^{-2}[2 - (1+\chi)^{1/2} - (1-\chi)^{1/2}], \tag{7}$$

$$\chi = \hbar\omega/E_0, \tag{8a}$$

$$\chi_{so} = \hbar\omega/(E_0+\Delta_0), \tag{8b}$$

where μ is the combined density-of-states mass and P is the momentum matrix element. In Eq. (5), the first and second terms in the curly bracket correspond to the free electron-hole pair contribution arising from the E_0 and $E_0 + \Delta_0$ gaps, respectively, and B corresponds to the higher-lying gaps contribution (same as $\epsilon_{1\infty}$). We assumed that the squared P-matrix elements have the same values between the E_0 and $E_0 + \Delta_0$ gap transitions since the detailed values are not well known at present. The parameters A and B can now be determined by fitting Eq. (5) with the experimental data. In the previous work,[15] we also found a simple relation that for a family of the III-V compounds (such as GaAs, InAs, InP, and GaP) the parameter A increases with increasing the band gap E_0 but decreases contrary with increasing E_0.

In order to test this model again, we made a least-square fit of the published dielectric-constant data of $Ga_{1-x}Al_xAs$ ternaries with the expression of Eq. (5). The result of this fit is shown in Fig. 1, where the figure shows the calculated curves of Eq. (5) (solid lines) along with the experimental data taken from Ref. (17) (open circles). The theoretical calculation requires only two material parameters, E_0 and Δ_0 gap energies. The dependence of the E_0 gap of the alloy $Ga_{1-x}Al_xAs$ on x, according to Afromowitz,[18] is given by

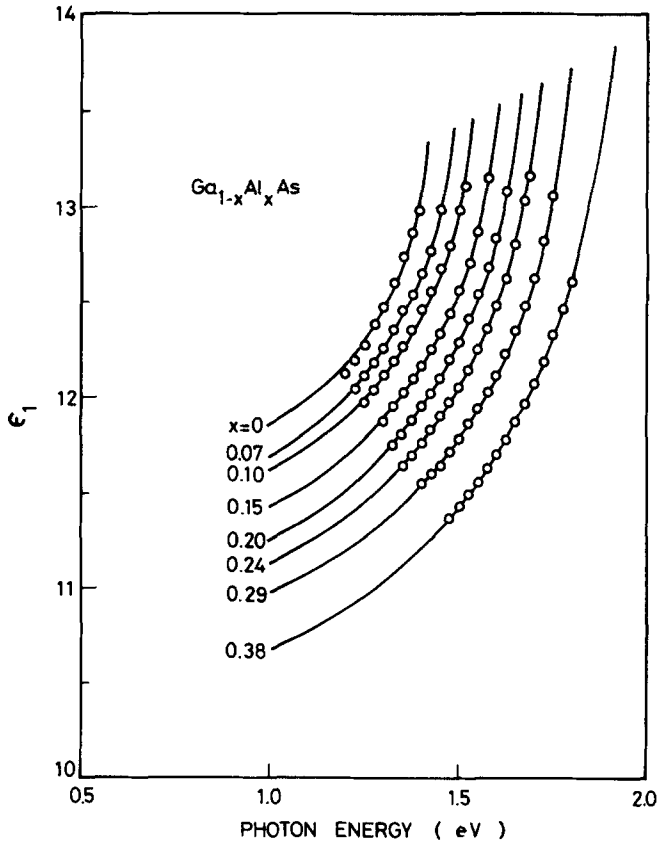

FIG. 1. Comparison of dielectric-constant data[17] and calculated results of this model for $Ga_{1-x}Al_xAs$ ternaries.

$$E_0(x) = 1.424 + 1.266x + 0.26x^2. \tag{9}$$

The compositional dependence of the Δ_0 (spin-orbit splitting) gap in the system may also be written as[19,20]

$$\Delta_0(x) = 0.34 - 0.5x. \tag{10}$$

As clearly seen in the figure, this comparison shows a quite good agreement between the calculation and experimental data. The numerical values of A and B, determined by fitting Eq. (5) with the experimental data, are shown in Fig. 2. The plots suggest the linear relation between the values of A (B) and Al content x, same as to the case for the $In_{1-x}Ga_xAs_yP_{1-y}$ quaternaries.[15] From a least-square-fit procedure, we obtain the relations

$$A(x) = 6.64 + 16.92x, \tag{11a}$$

$$B(x) = 9.20 - 9.22x. \tag{11b}$$

The dielectric constant $\epsilon_1(\omega)$ of the $Ga_{1-x}Al_xAs$ ternaries can then be specified in terms of x alone. Introducing Eqs. (9)–(11) into Eq. (5), one can easily calculate the spectral dependence of the dielectric constants in the alloy $Ga_{1-x}Al_xAs$ system with an optional composition x. The present result may, thus, useful for a variety of $Ga_{1-x}Al_xAs$ optoelectronic device applications.

B. Photoelastic coefficient

In this subsection, we shall present the theoretical expression of photoelastic coefficient in the III-V compounds. The investigation of the elasto-optic properties in

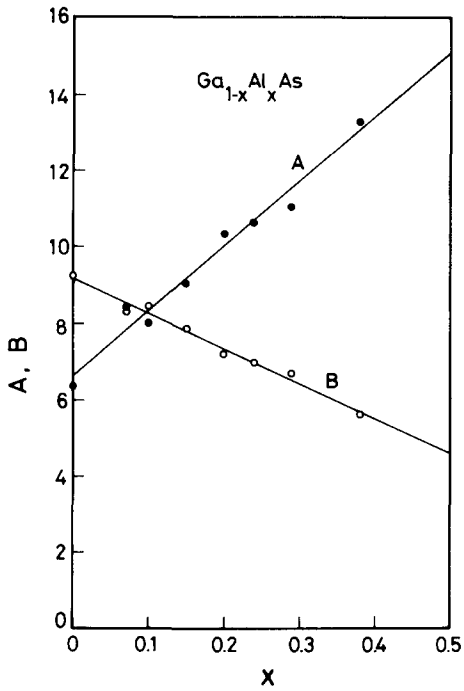

FIG. 2. Variation of A and B, required to fit this model [Eq. (5)] with the experimental data,[17] vs y for $Ga_{1-x}Al_xAs$ ternaries.

solids is an old topic of crystal optics.[1] The application of an external stress to a solid produces a change in its crystal symmetry and lattice parameters which results in significant changes in its optical properties. An optically isotropic semiconductor becomes birefringent under the action of external stress. The photoelastic coefficient α can be given by

$$\alpha = \frac{\Delta\epsilon_{ij}}{X} = -\sum_{mn} \epsilon_{ii}\,\epsilon_{jj}\,p_{ijkl}\,S_{klmn}, \tag{12}$$

where $\Delta\epsilon_{ij} = \epsilon_{\parallel} - \epsilon_{\perp}$ is the change in the real part of the dielectric constants parallel and perpendicular to the direction of the stress X, ϵ_{ii} (ϵ_{jj}) the component of the dielectric constant tensor in the absence of the stress, p_{ijkl} the component of the fourth-rank photoelastic tensor, and S_{klmn} is the component of the elastic compliance tensor. The first-order change in the real part of the dielectric constant $\Delta\epsilon_1^{DG}(\omega)$ with applied stress can be written as[10]

$$\Delta\epsilon_1^{DG}(\omega) = \sum_{i=A,B,C} \times\left(\frac{\partial\epsilon_1}{\partial M_i}\Delta M_i + \frac{\partial\epsilon_1}{\partial E_{gi}}\Delta E_{gi}\right), \tag{13}$$

where M ($=P^2$) is the squared P-matrix element, and the summation indicates that contributions from the three valence bands at Γ point must be included. The first and second terms on the right-hand side of Eq. (13) correspond to the contributions from the first-order change in the squared P-matrix elements and the interband transition energies, respectively. The stress-induced change in the real part of the dielectric constant $\Delta\epsilon_{1\infty}$ can also be expressed by a similar form as Eq. (13). The total stress-induced change $\Delta\epsilon_1(\omega)$ can, thus, be written as

$$\Delta\epsilon_1(\omega) = \Delta\epsilon_1^{DG}(\omega) + \Delta\epsilon_{1\infty}. \tag{14}$$

Introducing Eq. (5) into Eq. (13), one obtains finally the expression of the photoelastic coefficient:

$$\alpha = C\left\{-g(\chi) + \frac{4E_0}{\Delta_0} \times\left[f(\chi) - \left(\frac{E_0}{E_0+\Delta_0}\right)^{3/2} f(\chi_{s0})\right]\right\} + D, \tag{15}$$

with

$$C \begin{cases} = (\tfrac{2}{3}\mu)^{3/2}P^2 b\,(S_{11}-S_{12})\,E_0^{-5/2} \text{ for } X\|[100], & \text{(16a)} \\ = (\tfrac{2}{3}\mu)^{3/2}P^2 d S_{44} E_0^{-5/2}/2\sqrt{3} \text{ for } X\|[111], & \text{(16b)} \end{cases}$$

$$g(\chi) = \chi^{-2}[2-(1+\chi)^{-1/2}-(1-\chi)^{-1/2}], \tag{17}$$

where b and d are the shear deformation potentials of the valence band at Γ point. In Eq. (15), the first term corresponds to the dispersive contribution arising from the E_0 and $E_0+\Delta_0$ gaps and the second term D corresponds to the nondispersive contribution arising from other, far-off critical points in the band structure (same as $\Delta\epsilon_{1\infty}$). The parameters C and D can be determined by fitting Eq. (15) with the experimental data.

Let us now proceed to find some relations between the band-gap energy E_0 and best-fit parameters, C and D, for a number of the III-V compounds. The values of C versus E_0 for various III-V compounds are plotted in Fig. 3. Table I also shows the numerical values of C and D, required to least-square fit Eq. (15) with the experimental data, for various III-V compounds. One finds from the figure that the parameter C decreases asymptotically with increasing E_0, as can be expected from Eq. (16). The parameter D, on the other hand, does not exhibit such a simple relation, i.e., its value scatters by material to material (see Table I). This seems to be not so surprising. The nondispersive background contribution D arises from the higher-lying gaps (such as E_1, $E_1+\Delta_1$, and E_2 gaps). The contributions of the E_0, $E_1(E_1+\Delta_1)$, and E_2 gaps to the longer-wavelength α do not have the same signs. This sign is negative for E_0 and $E_1(E_1+\Delta_1)$ but posi-

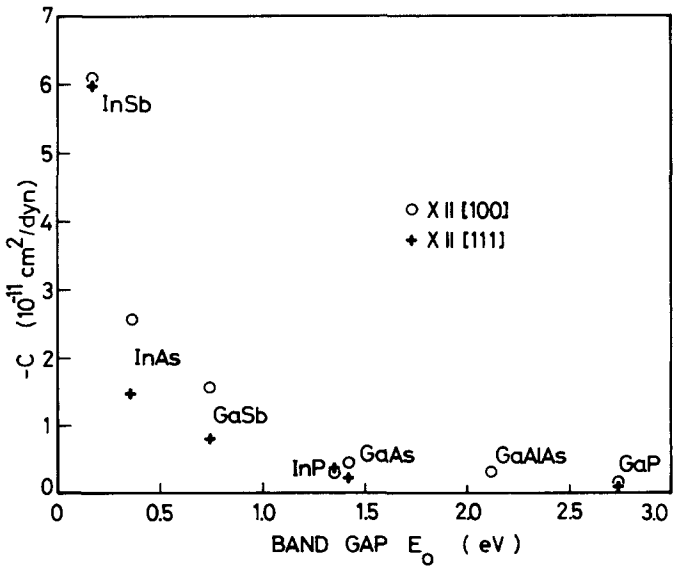

FIG. 3. Variation of C vs the direct-band gap E_0 for a family of the III-V compounds.

TABLE I. Values of C and D (in 10^{-11} cm^2/dyn) for several III-V compounds obtained by least-square fitting the experimental data of α with Eq. (15).

Material	C		D	
	$X \parallel [100]$	$X \parallel [111]$	$X \parallel [100]$	$X \parallel [111]$
InSb[a]	− 5.86	− 5.99	1.98	6.13
InAs[a]	− 2.58	− 1.48	2.19	2.32
GaSb[a]	− 1.56	− 0.85	3.74	4.14
InP[b]	− 0.29	− 0.36	1.39	2.60
GaAs[c]	− 0.46	− 0.21	2.22	2.12
GaAlAs[d]	− 0.32	...	1.35	...
GaP[b]	− 0.18	− 0.06	1.73	1.92

[a] P. Y. Yu, M. Cardona, and F. H. Pollak, Phys. Rev. B **3**, 340 (1971).
[b] F. Canal, M. Grimsditch, and M. Cardona, Solid State Commun. **29**, 523 (1979).
[c] C. W. Higginbotham, M. Cardona, and F. H. Pollak, Phys. Rev. **184**, 821 (1969).
[d] J. P. van der Ziel and A. C. Gossard, J. Appl. Phys. **48**, 3018 (1977).

tive for E_2 and they partially compensate each other.[13] This effect is thought to disturb some simple relations between D and E_0 for a family of the III-V compounds.

III. PHOTOELASTIC EFFECTS

A. $Ga_{1-x}Al_xAs$/GaAs heterostructure

This system is of particular interest because it has been employed to produce a wide variety of high-speed electron devices and optoelectronic ones. We consider a plane substrate of (001) surface orientation, i.e., the surface of which contains the xy plane of a Cartesian coordinate system (Fig. 4). Onto this substrate (GaAs) a thin layer ($Ga_{1-x}Al_xAs$) is deposited. The force resulting from the stress in the layer causes a deformation of the substrate and also of the film which remains attached to the surface of the substrate. The layer, as a result, would become birefringent. In this case, the lattice deformation of the layer can be explained by a strain field [e] of tetragonal symmetry[21]:

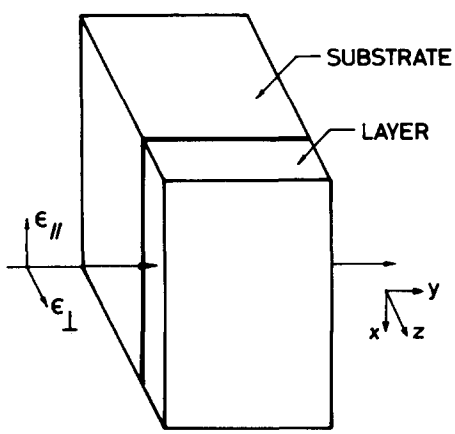

FIG. 4. Configuration of the system: thin layer: substrate.

$$[e] = \begin{bmatrix} e \\ e \\ -\frac{2C_{12}}{C_{11}} e \\ 0 \\ 0 \\ 0 \end{bmatrix}. \tag{18}$$

This strain field can be deduced to the "internal biaxial stress" parallel to the [100] and [010] directions.

To obtain the photoelastic coefficient, we need the magnitude of the applied stress [see Eq. (12)]. Investigations of an applied uniaxial stress in GaAs indicate that the excitons (or, more generally, interband transitions) undergo a splitting as well as a hydrostatic shift.[22] For compressive stress along the [100] axis, the lowest-energy exciton involves the light hole and the higher-energy exciton involves the heavy hole. One can obtain this stress-induced exciton energy shift, or vice versa the magnitude of the applied stress, from a calculation based on the orbital-strain Hamiltonian scheme.[23] This scheme can be successfully applied to the case for the internal-strain-deformed heteroepitaxial wafers.

Ziel and Gossard[24] have measured the energy difference ΔE between the light-hole and heavy-hole involved transitions to be 5.7 meV for $Ga_{0.5}Al_{0.5}As$ layer grown on (001)GaAs. By applying the orbital-strain Hamiltonian scheme,[23] we obtain the relation between the energy shift ΔE and stress X as

$$\Delta E = 2b\,(C_{11} - C_{12})^{-1} X. \tag{19}$$

For the $Ga_{0.5}Al_{0.5}As$ ternary, the tetragonal-symmetry deformation potential is estimated to be $b = -1.5$ eV [25] and the elastic stiffness constants are obtained to be $C_{11} = 12.19$ and $C_{12} = 5.36 \times 10^{11}$ dyn/cm^2.[26] The internal stress in the $Ga_{0.5}Al_{0.5}As$ epitaxial layer can then be estimated to be $X = 1.3 \times 10^9$ dyn/cm^2.

The calculated photoelastic coefficients of $Ga_{1-x}Al_xAs$ as a function of the photon energy with x-composition increments of 0.2 are shown in Fig. 5. The filled circles correspond to the data for GaAs taken from Ref. 10, and the open circles correspond to the data for $Ga_{1-x}Al_xAs$ ($x \simeq 0.5$) taken from Ref. 24. Ziel and Gossard[24] have measured the internal-stress-induced change in the refractive index $\Delta n = n_{\parallel} - n_{\perp}$ for $Ga_{0.5}Al_{0.5}As$ layer on GaAs substrate. To plot their data in Fig. 5, we required the following relation:

$$\Delta\epsilon = \epsilon_{\parallel} - \epsilon_{\perp} = \frac{1}{\alpha_r} \Delta n, \tag{20}$$

where α_r is the fractional coefficient defined by[27]

$$\alpha_r = \frac{1}{4}\left(\frac{\epsilon_1 + (\epsilon_1^2 + \epsilon_2^2)^{1/2}}{2}\right)^{-1/2} \times [1 + (\epsilon_1^2 + \epsilon_2^2)^{-1/2}\epsilon_1]. \tag{21}$$

In the region of transparency, i.e., $\epsilon_1 \gg \epsilon_2$, we can rightly reduce the coefficient to $\alpha_r \simeq \frac{1}{2}\epsilon_1^{-1/2}$. By least-square fitting these data with Eq. (15) and introducing a linear interpola-

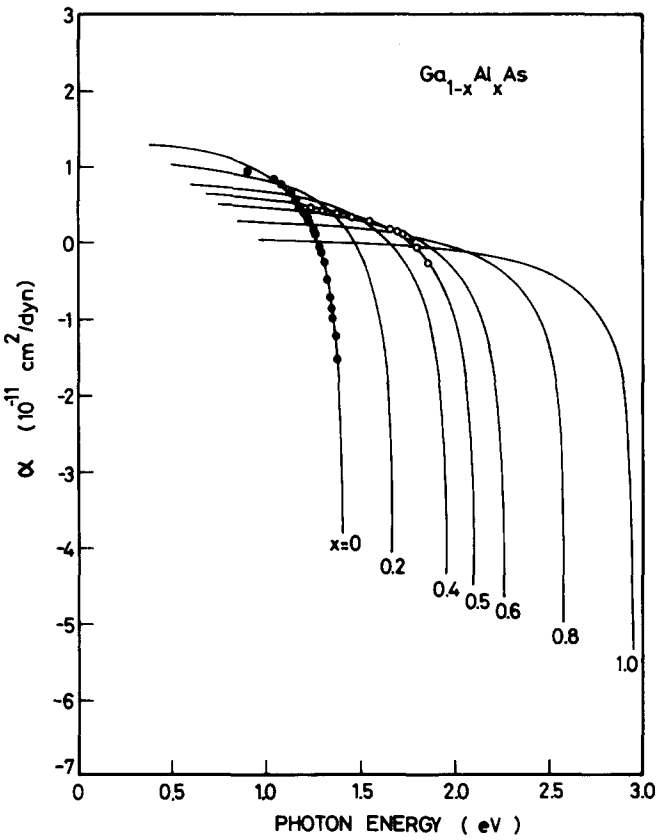

FIG. 5. Calculated photoelastic coefficients of $Ga_{1-x}Al_xAs$ as a function of the photon energy with x-composition increments of 0.2.

tion scheme, we obtain the following relation between $C(D)$ and Al content x:

$$C(x) = -0.46 + 0.28x, \tag{22a}$$

$$D(x) = 2.22 - 1.74x. \tag{22b}$$

We recognize from the figure that the photoelastic coefficient of $Ga_{1-x}Al_xAs$ has strong wavelength dispersion. The longer-wavelength photoelastic coefficient decreases with increasing Al content.

B. $In_{1-x}Ga_xAs_yP_{1-y}$/InP heterostructure

The calculation of the photoelastic coefficients in an alloyed system has been hampered by a lack of definite knowledge of many various material parameters, such as effective masses, elastic constant, and deformation potentials. An interpolation scheme is known to be a useful tool for estimating various parameters of alloys. The interpolation scheme is essentially based on known values for the related binary or ternary alloys. Although the interpolation scheme is still open to experimental verification, it provides more useful and reliable parameters over the entire range of alloy composition.[25] However, some kinds of material parameters, e.g., lattice thermal resistivity,[28] exhibit strong nonlinearity with respect to the alloy composition which arises from the effect of alloy disorder. In such a case, attention must be carefully paid to the interpolated values. The material parameters requiring for calculation of the photoelastic coefficients (i.e., effective masses, elastic constants, deformation potentials, etc.) could be well estimated by the linear interpolation scheme.[25] In this subsection, we try to obtain the wavelength dispersion of the photoelastic coefficients in a $In_{1-x}Ga_xAs_yP_{1-y}$ quaternary system by introducing a method of the linear interpolation scheme.

The III-V quaternary $In_{1-x}Ga_xAs_yP_{1-y}$ has been epitaxially grown on InP for the composition range of $0 \leqslant y \leqslant 1.0$,[29] provided

$$x = \frac{0.1894y}{0.4184 - 0.013y}. \tag{23}$$

The electronic band structures of this system have been studied by a number of groups. The E_0 and Δ_0 gaps for this system can be written as[29,30]

$$E_0(y) = 1.35\text{–}0.72y + 0.12y^2, \tag{24}$$

$$\Delta_0(y) = 0.12 + 0.3y + 0.11y^2. \tag{25}$$

Figures 6 and 7 show, respectively, the three-dimensional representations of the parameters C and D for $In_{1-x}Ga_xAs_yP_{1-y}$ over the entire range of compositions ($0 \leqslant x \leqslant 1.0$, $0 \leqslant y \leqslant 1.0$). The corners in the figures correspond to the values of the binaries determined in Sec. III. The bold lines in the figures are the loci of the values for compositions lattice-matched to InP. To obtain these figures, we used the following interpolation scheme[25]:

$$Q_{InGaAsP}(x,y) = (1-x)yB_{InAs} + (1-x)(1-y)B_{InP} + xyB_{GaAs} + x(1-y)B_{GaP}, \tag{26}$$

where $Q(x, y)$ is the quaternary parameter (C or D) and B's

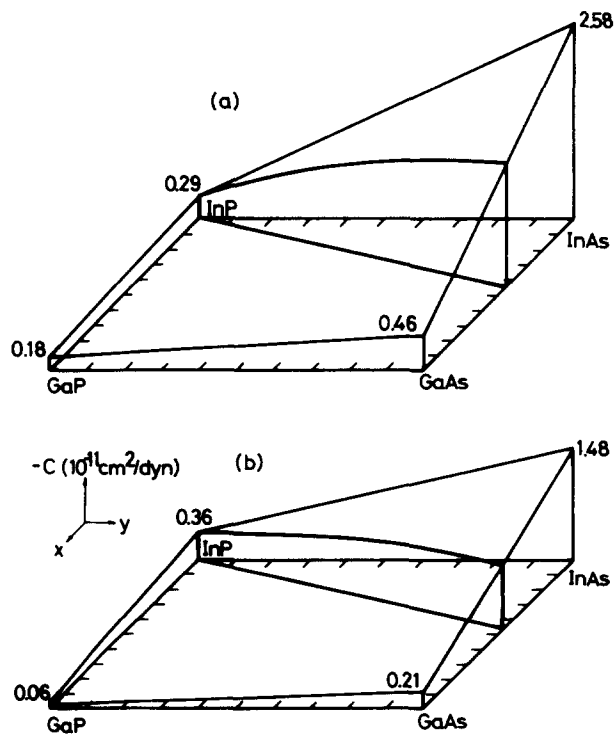

FIG. 6. Three-dimensional representations of the best-fit parameter C for $In_{1-x}Ga_xAs_yP_{1-y}$ over the entire range of compositions ($0 \leqslant y \leqslant 1.0$): (a) $X \| [100]$, (b) $X \| [111]$.

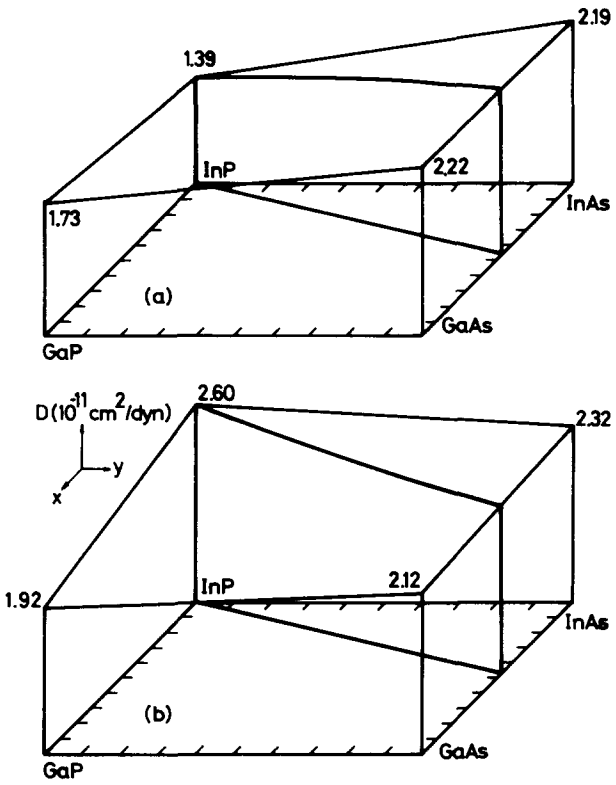

FIG. 7. Three-dimensional representations of the best-fit parameter D for $In_{1-x}Ga_xAs_yP_{1-y}$ over the entire range of compositions ($0<y<1.0$): (a) $X \| [100]$, (b) $X \| [111]$.

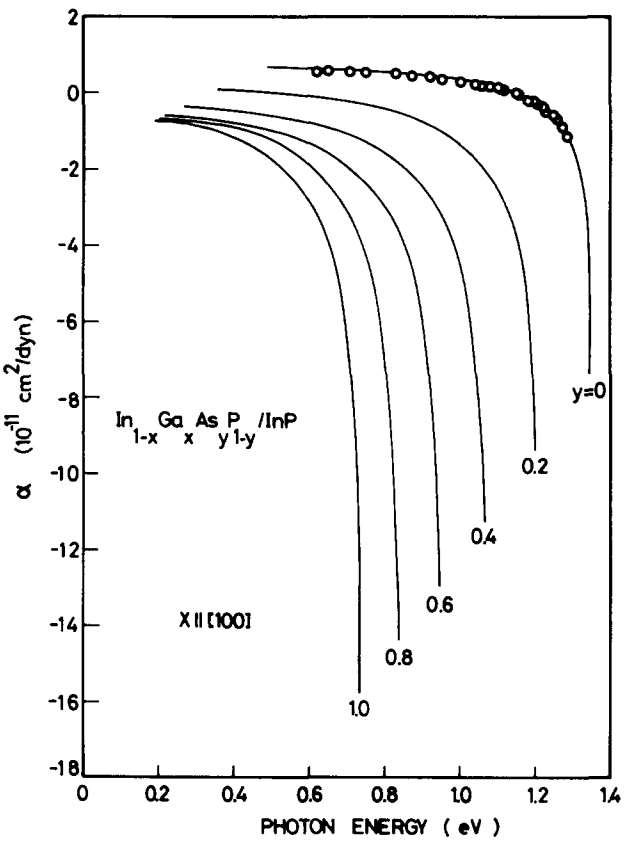

FIG. 8. Calculated photoelastic coefficients of $In_{1-x}Ga_xAs_yP_{1-y}$ for $X \| [100]$ as a function of the photon energy with y-composition increments of 0.2.

are the corresponding binary parameters (see Table I). As mentioned in Sec. III, the parameter C has the largest value for the smallest E_0-gap material, i.e., InAs (see Fig. 7). The parameter D, on the other hand, does not show such a simple relation with the E_0-gap energy (see Fig. 8).

From the above arguments, the photoelastic coefficients of $In_{1-x}Ga_xAs_yP_{1-y}$ can be specified in terms of y alone. Introducing Eqs. (23)–(26) into Eq. (15), we can present the spectral dependence of the photoelastic coefficients of $In_{1-x}Ga_xAs_yP_{1-y}$ lattice-matched to InP. The calculated photoelastic coefficients of this system as a function of the photon energy with y-composition increments of 0.2 for the case of the stress parallel to the [100] axis are shown in Fig. 8. This result corresponds to the configuration of Fig. 4, i.e., corresponds to the photoelastic coefficients of internal-strain-deformed $In_{1-x}Ga_xAs_yP_{1-y}$ layers grown on (001)InP substrates. The calculated coefficients for the case of the stress parallel to the [111] axis are also shown in Fig. 9. In this case, the calculated results correspond to the case for internal-strain-deformed $In_{1-x}Ga_xAs_yP_{1-y}$ layers grown on (111)InP substrates. The $In_{1-x}Ga_xAs_yP_{1-y}$ layers grown on (111)InP substrates have internal strains of the rhombohedral symmetry. The internal-strain-induced change in the dielectric constant can, thus, be explained in terms of the rhombohedral-symmetry deformation potential d [see Eq. (16b)]. The open circles in the figures are the experimental data of InP taken by Canal *et al.*[12]

Figure 10 shows the isotropic point versus composition y of $In_{1-x}Ga_xAs_yP_{1-y}$ quaternaries for both the [100] and

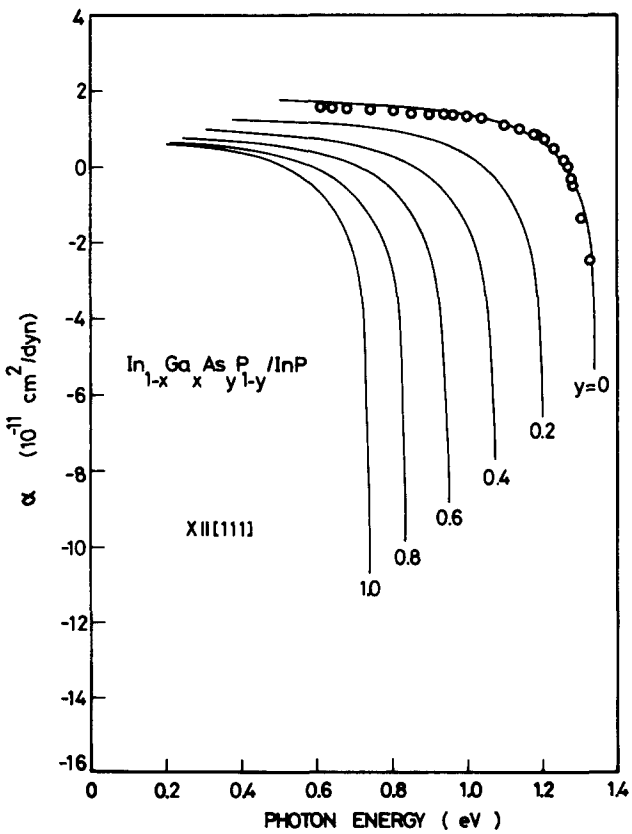

FIG. 9. Calculated photoelastic coefficients of $In_{1-x}Ga_xAs_yP_{1-y}$ for $X \| [111]$ as a function of the photon energy with y-composition increments of 0.2.

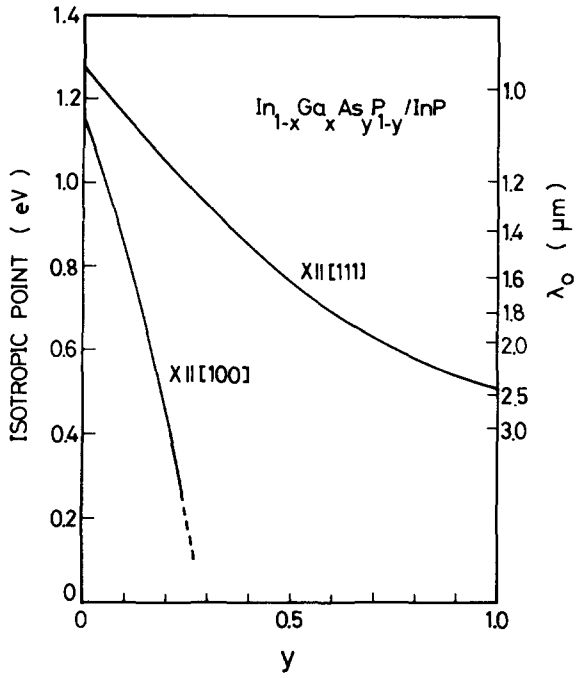

FIG. 10. Isotropic point vs composition y for $In_{1-x}Ga_xAs_yP_{1-y}/InP$ system.

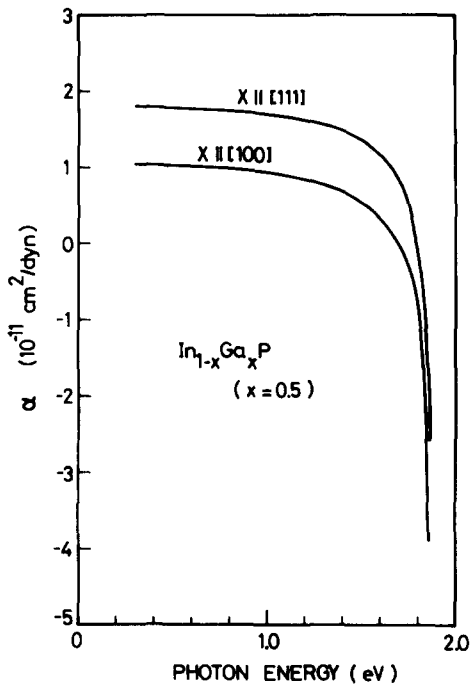

FIG. 11. Calculated photoelastic coefficients for $In_{0.5}Ga_{0.5}P$ lattice-matched to GaAs.

[111] stresses. The isotropic point occurs at the photon energy corresponding

$$\Delta\epsilon_1(\omega) = \Delta\epsilon_1^{DG}(\omega) + \Delta\epsilon_{1\infty} = 0, \tag{27}$$

i.e., it occurs at which the lowest-gap contribution $\Delta\epsilon_1^{DG}(\omega)$ is cancelled by the higher-lying gaps contribution $\Delta\epsilon_{1\infty}$. The isotropic point means, in other words, that at this photon energy the strain-deformed layer still remains optically isotropic in nature.

By applying the present procedure, one can also easily estimate the spectral dependence of the photoelastic coefficients of $In_{1-x}Ga_xAs_yP_{1-y}$ alloys with optional (x, y) contents. Figure 11 shows, as an example, the photoelastic coefficients of $In_{1-x}Ga_xP$ layer ($x \simeq 0.5$, $y = 0$) lattice-matched to GaAs. This system has been extensively studied as a potential material for visible optoelectronic device applications. The curves are obtained from Eq. (15) with the following numerical values: $E_0 = 1.87$ eV; $E_0 + \Delta_0 = 1.98$ eV; $C = -0.24$ and $D = 1.56\times10^{-11}$ cm^2/dyn for $X\|[100]$; and $C = -0.21$ and $D = 2.26\times10^{-11}$ cm^2/dyn $X\|[111]$. From this figure, one can expect the isotropic points to be occur at 1.7 eV for the [100] stress and at 1.8 eV for the [111] stress.

IV. CONCLUSION

Photoelastic coefficients of III-V compounds have been analyzed with a theoretical prediction based on a simplified model of the interband transitions. The theoretical expression requires two parameters: C arising from the lowest-gap contribution and D arising from the higher-lying gaps contribution. A least-square fitting procedure of the theoretical prediction with the experimental data of various III-V compounds indicates that the parameter C increases with increasing the lowest-direct gap E_0 but D does not show such a simple relation. The analysis has been successfully applied to obtain the spectral dependence of the photoelastic coefficients of $Ga_{1-x}Al_xAs$ lattice-matched to GaAs and $In_{1-x}Ga_xAs_yP_{1-y}$ lattice-matched to InP. A method for analysis of the internal-strain induced effects in elastically-deformed heterostructure crystals is also discussed in detail.

ACKNOWLEDGMENTS

The authors wish to thank K. Kumabe, S. Shimada, and N. Kuroyanagi for their continual encouragement.

[1] J. F. Nye, *Physical Properties of Crystals* (Clarendon, Oxford, 1972).
[2] G. H. Olsen and M. E. Ettenberg, in *Crystal Growth: Theory and Techniques*, edited by C. H. L. Goodman (Plenum, New York, 1978), Vol. 2.
[3] F. K. Reinhart and R. A. Logan, J. Appl. Phys. **44**, 3171 (1973).
[4] K. Röll, J. Appl. Phys. **47**, 3224 (1976).
[5] S. Kishino, N. Chinone, H. Nakashima, and R. Ito, Appl. Phys. Lett. **29**, 488 (1976).
[6] G. H. Olsen and M. Ettenberg, J. Appl. Phys. **48**, 2543 (1977).
[7] P. A. Kirkby, P. R. Selway, and L. D. Westbrook, J. Appl. Phys. **50**, 4567 (1979).
[8] R. W. Dixon, J. Appl. Phys. **38**, 5149 (1967).
[9] A. Ferdman and D. Horowitz, J. Appl. Phys. **39**, 5597 (1968).
[10] C. H. Higginbotham, M. Cardona, and F. H. Pollak, Phys. Rev. **184**, 821 (1969).
[11] L. N. Glurdzhidze, A. P. Izergin, Z. N. Kopylova, and A. D. Remenyuk, Sov. Phys.-Semicond. 7, 305 (1973).
[12] F. Canal, M. Grimsditch, and M. Cardona, Solid State Commun. **29**, 523 (1979).
[13] P. Y. Yu, M. Cardona, and F. H. Pollak, Phys. Rev. B **3**, 340 (1971).
[14] A. Y. Shileika, M. Cardona, and F. H. Pollak, Solid State Commun. 7, 1113 (1969).
[15] S. Adachi, J. Appl. Phys. **53**, 5863 (1982).
[16] F. Abelès, *Optical Properties of Solids* (North-Holland, Amsterdam, 1972).

[17]H. C. Casey, Jr., D. D. Sell, and M. B. Panish, Appl. Phys. Lett. **24**, 63 (1974).
[18]M. A. Afromowitz, Solid State Commun. **15**, 59 (1974).
[19]M. Cardona, K. L. Shaklee, and F. H. Pollak, Phys. Rev. **154**, 696 (1967).
[20]R. Braunstein and E. O. Kane, J. Phys. Chem. Solids **23**, 1423 (1962).
[21]H. Asai and K. Oe, J. Appl. Phys. **54**, 2052 (1983).
[22]D. D. Sell, S. E. Stokowski, R. Dingle, and J. V. DiLorenzo, Phys. Rev. B **7**, 4568 (1973).
[23]F. H. Pollak and M. Cardona, Phys. Rev. **172**, 816 (1968).
[24]J. P. van der Ziel and A. C. Gossard, J. Appl. Phys. **48**, 3018 (1977).
[25]S. Adachi, J. Appl. Phys. **53**, 8775 (1982).
[26]These values were obtained from a linear interpolation scheme between the values $C_{11} = 11.9$ and $C_{12} = 5.38 \times 10^{11}$ dyn/cm^2 for GaAs [K. Fletcher and P. N. Butcher, J. Phys. C **5**, 212 (1972)] and $C_{11} = 12.5$ and $C_{12} = 5.34 \times 10^{11}$ dyn/cm^2 for AlAs [J. D. Wiley, in *Semiconductors and Semimetals*, edited by R. K. Willardson and A. C. Beer (Academic, New York, 1975), Vol. 10].
[27]S. Adachi and C. Hamaguchi, Phys. Rev. B **21**, 1701 (1980).
[28]S. Adachi, J. Appl. Phys. **54**, 1844 (1983).
[29]R. E. Nahory, M. A. Pollack, W. D. Johnston, Jr., and R. L. Barns, Appl. Phys. Lett. **33**, 659 (1978).
[30]E. H. Perea, E. E. Mendez, and C. G. Fonstad, Appl. Phys. Lett. **36**, 978 (1980).